An Empirical Correlation between Amide Deuterium Isotope Effects on $^{13}C^{\alpha}$ Chemical Shifts and Protein Backbone Conformation

Marcel Ottiger and Ad Bax*

Contribution from the Laboratory of Chemical Physics, National Institute of Diabetes and Digestive and Kidney Diseases, National Institutes of Health, Bethesda, Maryland 20892-0520

Received March 10, 1997. Revised Manuscript Received June 12, 1997[⊗]

Abstract: Three-dimensional, triple resonance NMR techniques are described for measurement of two-bond (intraresidual) and three-bond (sequential) amide deuterium isotope effects on $^{13}C^{\alpha}$ chemical shifts. Measurements were carried out for uniformly ^{15}N and ^{13}C labeled human ubiquitin equilibrated in a 50% H_2O/50% D_2O mixed solvent. The three-bond isotope shift, $^3\Delta C^{\alpha}(ND)$, ranges from about 10−50 ppb, and, except for residues with positive ϕ angles and residues followed by Gly, its magnitude is described by $^3\Delta C^{\alpha}(ND) = 30.1 + 22.2 \sin(\psi) \pm 3.4$ ppb. The two-bond isotope shift, $^2\Delta C^{\alpha}(ND)$, ranges from 70 to 116 ppb and is also dominated by the local backbone geometry at the C^{α} position: $^2\Delta C^{\alpha}(ND) = 93.1 + 10.1 \sin(\phi+62°) + 12.0 \sin(\psi+42°) \pm 4.1$ ppb.

Deuterium isotope effects on chemical shifts in NMR have been extensively studied over the past two decades[1−13] and have proven to be useful for spectral assignment and structure determination of small organic molecules. It is now generally established that isotope shift effects are vibrational in origin: the lower zero-point vibrational energy of the heavier isotopomer and the anharmonicity of the bond stretching potential curve results in a shorter average internuclear separation of the heavier isotopomer.[7,10] The magnitude of the isotope effect on nuclear magnetic shielding is governed by a variety of factors, including the number of bonds between the observed nucleus and the position of the isotopic substitution, conformation, hybridization, substituents, and hydrogen bonding. However, understanding of these factors remains incomplete, especially concerning effects over more than two bonds. Reasonable agreement between experimentally observed isotope effects and *ab initio* results so far has only been obtained for very simple model compounds.[7]

An empirical treatment is therefore inevitable and may contribute to a better understanding of the physical origin of the effect. In previous empirical studies it was reported that the magnitude of the deuterium isotope effects over two bonds is related to the strength of the hydrogen bond donated by NH/D.[11,12] It was also found that the three-bond isotope effects depend on the dihedral angle formed by the corresponding bonds, similar to a Karplus relationship.[5,9,11] Taking advantage of the fact that NH protons in peptide bonds exchange, but relatively slowly, a deuterium isotope effect on the ^{13}C chemical shifts of carbons in or near peptide bonds can readily be observed in molecules examined in a H_2O/D_2O solvent mixture. Applications have been reported for the carbonyl carbons in peptides[1,14] and proteins.[11,15,16]

Recent renewed interest in deuteration of proteins has been fueled by its potential to yield longer ^{13}C relaxation times, thereby extending the size limit of proteins that can be studied in detail by high resolution NMR.[17−20] Although the intrinsic utility of one-bond $^{13}C^{\alpha}$-{$^1H/^2H$} deuterium isotope shifts, $^1\Delta C^{\alpha}(D)$, for determining backbone geometry has been recognized,[13] effects over two and three bonds generally are considered a nuisance as they broaden the width of ^{13}C resonances in cases of incomplete deuteration. Variations observed in the magnitude of the isotope shifts also make it more difficult to correlate ^{13}C chemical shifts in a protonated protein with those in the perdeuterated counterpart.[21,22] However, with improved understanding of the origin of these isotope shifts, they potentially can become useful as reporters for side-chain geometry.

Here, we present the first report of amide deuterium isotope effects on $^{13}C^{\alpha}$ chemical shifts in a protein, human ubiquitin,

[⊗] Abstract published in *Advance ACS Abstracts,* August 1, 1997.

(1) Feeney, J.; Partington, P.; Roberts, G. C. K. *J. Magn. Reson.* **1974**, *13*, 268−274. Hawkes, G. E.; Randall, E. W.; Hull, W. E.; Gattegno, D.; Conti, F. *Biochemistry* **1978**, *17*, 3986−3992.

(2) Wehrli, F. W.; Wirthlin, T. *Interpretation of Carbon-13 NMR Spectra*; Heyden: London, 1976.

(3) Majerski, Z.; Zuanic, M.; Metelko, B. *J. Am. Chem. Soc.* **1985**, *107*, 1721−1726.

(4) Reuben, J. *J. Am. Chem. Soc.* **1985**, *107*, 1747−1755 and references therein.

(5) Yashiro, M.; Shigenobu, Y.; Yoshikawa, S. *J. Am. Chem. Soc.* **1986**, *108*, 1096−1097.

(6) Henry, G. D.; Weiner, J. H.; Sykes, B. D. *Biochemistry* **1987**, *26*, 3626−3634.

(7) Hansen, P. E. *Prog. NMR Spectrosc.* **1988**, *20*, 207−255.

(8) Tüchsen, E.; Hansen, P. E. *Biochemistry* **1988**, *27*, 8568−8576.

(9) Aydin, R.; Frankmölle, W.; Schmalz, D.; Günther, H. *Magn. Reson. Chem.* **1988**, *26*, 408−411.

(10) Berger, S. In *NMR, Basic Principles and Progress*; Günther, H., Ed.; Springer: Berlin, 1990; Vol. 22, pp 2−28.

(11) Tüchsen, E.; Hansen, P. E. *Int. J. Biol. Macromol.* **1991**, *13*, 2−8.

(12) Hansen, P. E.; Kolonicny, A.; Lycka, A. *Magn. Reson. Chem.* **1992**, *30*, 786−795.

(13) LeMaster, D. M.; LaIuppa, J. C.; Kushlan, D. M., *J. Biomol. NMR* **1994**, *4*, 863−870.

(14) Otter, A.; Liu, X.; Kotovych, G. *J. Magn. Reson.* **1990**, *86*, 657−662.

(15) Kainosho, M.; Nagao, H.; Tsuji, T. *Biochemistry* **1987**, *26*, 1068−1075.

(16) Henry, G. D.; Weiner, J. H.; Sykes, B. D. *Biochemistry* **1987**, *26*, 3626−3634.

(17) Grzesiek, S.; Anglister, J.; Ren, H.; Bax, A. *J. Am. Chem. Soc.* **1993**, *115*, 4369−4370.

(18) Shan, X.; Gardner, K. H.; Muhandiram, D. R.; Rao, N. S.; Arrowsmith, C. H.; Kay, L. E. *J. Am. Chem. Soc.* **1996**, *118*, 6570−6579.

(19) Smith, B. O.; Ito, Y.; Raine, A.; Techmann, S.; Ben-Tovim, L.; Nietlispach, D.; Broadhurst, R. W.; Terada, T.; Kelly, M.; Oschkinat, H.; Shibata, T.; Yokoyama, S.; Laue, E. D. *J. Biomol. NMR* **1996**, *8*, 360−368.

(20) Farmer II, B. T.; Venters, R. A. *J. Am. Chem. Soc.* **1995**, *117*, 4187−4188.

(21) Venters, R. A.; Farmer II, B. T.; Fierke, C. A.; Spicer, L. D. *J. Mol. Biol.* **1996**, *264*, 1101−1116.

(22) Garrett, D. S.; Seok, Y.-J.; Lee, B. R., Gronenborn; A. M.; Clore, G. M. *Biochemistry* **1997**, *36*, 861−872.

S0002-7863(97)00746-4 CCC: $14.00

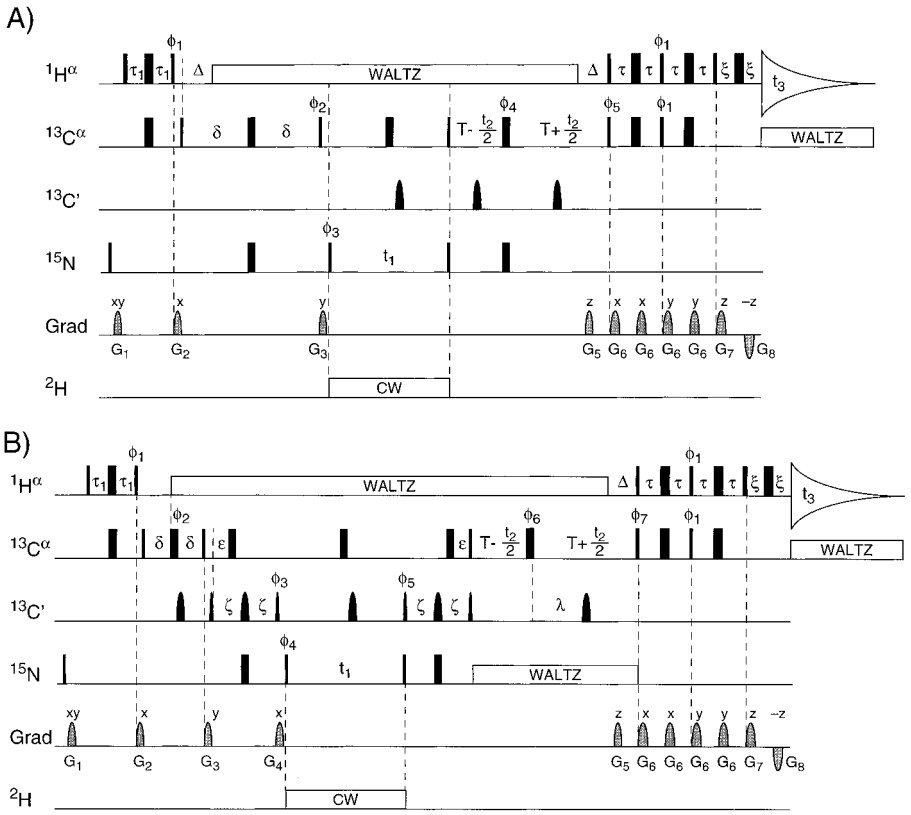

Figure 1. Pulse schemes of the gradient-enhanced 3D HCAN (A) and HCA(CO)N (B) experiments. Narrow and wide pulses correspond to 90° and 180° flip angles, respectively. Pulses for which the phase is not indicated are applied along the *x*-axis. The ^{1}H carrier is placed at the H_2O frequency. Broadband decoupling is accomplished with synchronous (^{1}H, ^{15}N) or asynchronous ($^{13}C^{\alpha}$) WALTZ16 sequences; ^{2}H decoupling is applied in the continuous-wave mode, using a 1.25 kHz RF field centered at 8 ppm. The carriers for the $^{13}C^{\alpha}$ and $^{13}C'$ pulses are positioned at 57.5 and 176 ppm, respectively. The power levels of the 90° and 180° $^{13}C^{\alpha}$ pulses, 4.6 and 10.3 kHz, respectively, at 151 MHz ^{13}C frequency, are adjusted such that they do not excite the $^{13}C'$ nuclei. Carbonyl pulses have a shaped amplitude profile, corresponding to the center lobe of a sin *x*/*x* function, and a duration of 96 μs for the 90° pulse. Phase cycling is as follows: (A) $\phi_1 = y$; $\phi_2 = 4(x),4(-x)$; $\phi_3 = x,x,-x,-x$; $\phi_4 = x,y,-x,-y$; Acq. $= x,2(-x),x,-x,2(x),-x$ and (B) $\phi_1 = y$; $\phi_2 = 348°$; $\phi_3 = 4(55°)$, $4(235°)$; $\phi_4 = 2(x),2(-x)$; $\phi_5 = 305°$; $\phi_6 = 348°$, 78°, 168°, 258°; Acq. $= x,-x,-x,x,-x,x,x,-x$. Quadrature detection in the t_1 dimension is obtained by changing the phases ϕ_3 (A) and ϕ_4 (B) in the usual States-TPPI manner. Quadrature detection in the t_2 dimension is obtained by inverting the polarity of G_5 together with ϕ_5 (A) and ϕ_7 (B), with data stored separately, in order to obtain Rance−Kay style data.[29] Delay durations for (A) are $\tau_1 = 1.5$, $\tau = 1.7$, $\Delta = 3.4$, $\delta = 14.28$, and $T = 14.28$ ms; for (B): $\tau_1 = 1.5$, $\tau = 1.7$, $\Delta = 3.4$, $\xi = 0.5$, $\delta = 3.3$, $\epsilon = 4.5$, $\zeta = 13.1$, $\lambda = 9.73$, and $T = 14.28$ ms. All pulsed field gradients (Grad) have sine-bell shaped amplitude profiles with a strength of 25 *G*/cm at their center and durations $G_{1,2,3,4,5,6,7,8} = 5.0$, 1.5, 0.7, 0.5, 1.56, 0.5, 0.25, and 0.15 ms. Pulse sequence code for Bruker DMX spectrometers has been deposited with the BioMagResBank at Madison, WI.

and correlate our experimental observations with the local geometry of the protein backbone in the crystal structure.[23] Results show that the three-bond amide deuterium isotope shift, $^{3}\Delta C^{\alpha}(ND)$, depends primarily on the backbone angle ψ. Remarkably, ψ is not the dihedral angle formed by the atoms involved in this effect but determines the position of the amide hydrogen relative to the substituents on the preceding $^{13}C^{\alpha}$. The two-bond isotope shift, $^{2}\Delta C^{\alpha}(ND)$, depends on ϕ and ψ, and, counter to predictions,[11,12] it tends to show a small *decrease* in magnitude with increasing strength of the hydrogen bond donated by the amide hydrogen.

Experimental Section

All NMR experiments were carried out at 30 °C on a sample of commercially obtained uniformly $^{13}C/^{15}N$-enriched human ubiquitin (VLI Research, Southeastern, PA; 1.5 mM in 50% H_2O/50% D_2O, 30 mM sodium acetate, pH* 4.7, 220 μl in a Shigemi microcell). All spectra were recorded on a Bruker DMX-600 spectrometer, equipped with a triple resonance, three-axis pulsed field gradient probehead. Spectra were processed using the NMRPipe software package,[24] and peak positions were determined by contour averaging using the program PIPP,[25] as described previously.[26] Resonance assignments were taken from Wang *et al.*[27] In order to obtain estimates for the random error in each of the measurements, all spectra were recorded twice.

The HCAN spectrum for measurement of $^{2}\Delta C^{\alpha}(ND)$ and the HCA(CO)N spectrum for measurement of $^{3}\Delta C^{\alpha}(ND)$ were recorded as 3D data matrices of 40* × 48* × 512* complex points (*n** denotes *n* complex points), with acquisition times of 47.0 (t_1, ^{15}N), 28.6 (t_2, $^{13}C^{\alpha}$), and 85.2 ms (t_3, ^{1}H). Both spectra were first recorded with pulse sequences very similar to the 2D versions of these experiments described by Wang *et al.*[27] (Figure 1, Supporting Information) and subsequently with the pulse sequences of Figure 1. These latter experiments use Rance−Kay style[28,29] gradient-enhanced quadrature detection in the $^{13}C^{\alpha}$ dimension, which results in improved sensitivity and a higher level of solvent signal suppression. The measuring time was 25 h for each 3D spectrum. Acquired data were apodized with a 81°-shifted squared sine-bell in the t_3 dimension, truncated at 0.4% ($\sin^2$ 176°) at the end of the FID, with a 72°-shifted sine-bell in the t_1

(23) Vijay-Kumar, S.; Bugg, C. E.; Cook, W. J. *J. Mol. Biol.* **1987**, *194*, 531−544.
(24) Delaglio, F.; Grzesiek, S.; Vuister, G. W.; Zhu, G.; Pfeifer, J.; Bax, A. *J. Biomol. NMR* **1995**, *6*, 277−293.
(25) Garret, D. S.; Powers, R.; Gronenborn, A. M.; Clore, G. M. *J. Magn. Reson.* **1991**, *95*, 214−220.
(26) Wang, A. C.; Bax, A. *J. Am. Chem. Soc.* **1996**, *118*, 2483−2494.
(27) Wang, A. C.; Grzesiek, S.; Tschudin, R.; Lodi, P. J.; Bax, A. *J. Biomol. NMR* **1995**, *5*, 376−382.
(28) Palmer III, A. G.; Cavanagh, J.; Wright, P. E.; Rance, M. *J. Magn. Reson.* **1991**, *93*, 151−170.
(29) Kay, L. E.; Keifer, P.; Saarinen, T. *J. Am. Chem. Soc.* **1992**, *114*, 10663−10665.

dimension, truncated at 6% (sin 176°) and, after extending the data with mirror-image linear prediction[30] (eight coefficients) to 1.5 times the recorded data size, with a 81°-shifted squared sine-bell in the t_2 dimension, truncated at 0.4%. Data were zero filled prior to Fourier transformation to yield a digital resolution of 3.3 (F_1), 3.3 (F_2), and 5.9 Hz (F_3) in the final spectrum.

Amide deuterium isotope effects on protein $^{13}C^{\alpha}$ chemical shifts are defined as ${}^{n}\Delta C^{\alpha}(ND) = \delta C^{\alpha}(H) - \delta C^{\alpha}(D)$, where n denotes the number of bonds between the C^{α} observed and the position of the isotopic NH/D substitution, and δC^{α} is the $^{13}C^{\alpha}$ chemical shift.[7] Optimal fits between the observed isotope shifts and backbone torsion angles were calculated using the least squares method as implemented in the program MATHEMATICA (Wolfram Inc., Champaign, IL).

Results

Measurement of $^{2}\Delta C^{\alpha}(ND)$ and $^{3}\Delta C^{\alpha}(ND)$. The principal problems with measurement of isotope shifts over multiple bonds in proteins have been the small magnitude of these effects relative to the natural line width, and the high degree of resonance overlap in proteins. In the present study we solve the spectral crowding problem by dispersing the NMR spectrum in three-dimensional frequency space. The line width problem is solved by separating the $^{13}C^{\alpha}$-{NH} and $^{13}C^{\alpha}$-{ND} resonances in an orthogonal dimension (^{15}N) of the spectrum, in a manner fully analogous to heteronuclear E. COSY experiments, where the large one-bond heteronuclear coupling is used to resolve the much smaller multibond J couplings.[31−34] Here, it is the large one-bond isotope shift [$^{1}\Delta N(D) \approx 0.65$ ppm] which is used to separate correlations to ^{15}N-{H} and ^{15}N-{D} in the 3D NMR spectrum.

In the present study, we use 3D HCAN and 3D HCA(CO)N experiments for measurement of $^{2}\Delta C^{\alpha}(ND)$ and $^{3}\Delta C^{\alpha}(ND)$, respectively (Figure 1). These experiments have been described previously,[27] and only minor modifications are used in the present study. First, the experiment is carried out in a 3D instead of a 2D manner, and the duration of this additional, constant-time evolution period is set to $1/^{1}J_{C\alpha C\beta} \approx 28$ ms. Second, Rance−Kay style gradient-enhanced quadrature detection is used in the $^{13}C^{\alpha}$ dimension, resulting in improved sensitivity and solvent signal suppression.[29] Spectra have also been recorded without gradient-enhanced quadrature detection, and details regarding these pulse sequences and corresponding parameters are included as Supporting Information.

Figure 2 shows cross sections, taken orthogonal to the F_3 axis at $F_3 = 4.51$ ppm, through the HCAN and HCA(CO)N spectra of uniformly $^{13}C/^{15}N$-enriched human ubiquitin. The HCAN spectrum (Figure 2A) correlates H^{α}_i with $^{13}C^{\alpha}_i$ and with $^{15}N_i$ and $^{15}N_{i+1}$. The correlations to $^{15}N_i$ and $^{15}N_{i+1}$ are based on magnetization transfer through $^{1}J_{NC}{}^{\alpha}$ and $^{2}J_{NC}{}^{\alpha}$, respectively, and as $^{2}J_{NC}{}^{\alpha}$ on average is considerably smaller than $^{1}J_{NC}{}^{\alpha}$,[35] the correlations to $^{15}N_{i+1}$ are correspondingly weaker. The HCA(CO)N spectrum correlates H^{α}_i with $^{13}C^{\alpha}_i$ and exclusively with $^{15}N_{i+1}$ and yields higher sensitivity than the HCAN experiment. As the protein has been equilibrated in 50% H_2O/50% D_2O, all backbone ^{15}N nuclei (except Pro) show a doublet-like splitting. The one-bond isotope shift, $^{1}\Delta N(D)$, is known to be positive, and the upfield ^{15}N resonance corresponds to the ^{15}ND isotopomer, and the downfield one to ^{15}NH. As the ^{15}ND isotopomer also corresponds to an upfield $^{13}C^{\alpha}$ shift in the spectra of Figure 2, this establishes the sign of $^{2}\Delta C^{\alpha}(ND)$ and $^{3}\Delta C^{\alpha}(ND)$ to be positive. The relative intensity of the two doublet components reflects the equilibrium isotope fractionation but is also influenced by different relaxation rates in the two isotopomers.[36]

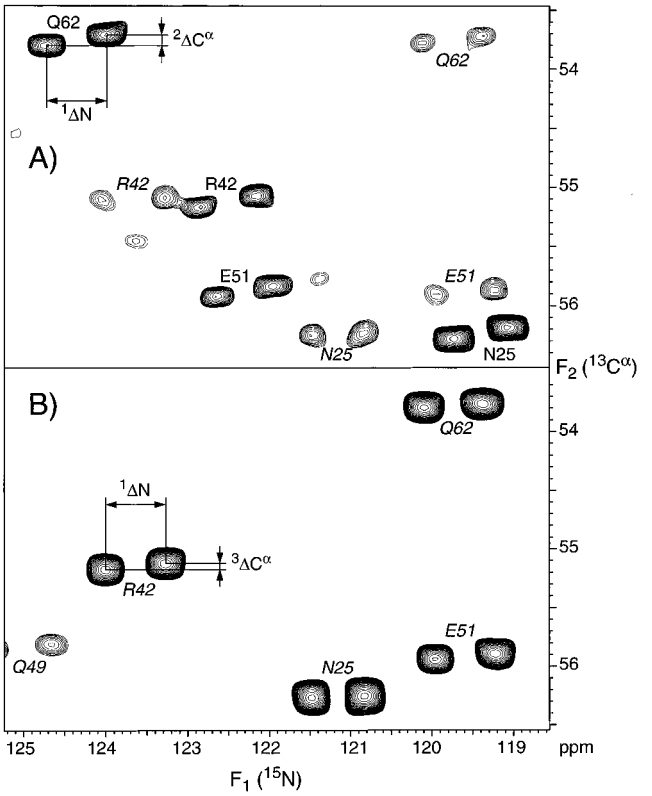

Figure 2. Sections of [$F_1(^{15}N)$,$F_2(^{13}C^{\alpha})$]-planes, taken at $F_3(^{1}H) = 4.51$ ppm of (A) the 3D HCAN and (B) the HCA(CO)N spectra of human ubiquitin in 50% H_2O/50% D_2O. Resonances are labeled with the amino acid type and residue number of the corresponding C^{α} carbon, where regular and italic numbers denote correlations to the intraresidual and sequential ^{15}N, respectively.

As the ^{15}N is subject to a large one-bond isotope shift, $^{1}\Delta N$-(D), the $^{13}C^{\alpha}$ signals correlated with $^{15}N(H)$ and $^{15}N(D)$ are displaced relative to one another in the ^{15}N dimension of the 3D spectrum by this one-bond isotope shift. Thus, the small multibond isotope shift effects are resolved by virtue of the much larger one-bond isotope shift (Figure 2). This makes it possible to measure accurately the much smaller relative displacements of the two doublet components in the $^{13}C^{\alpha}$ dimension, which correspond to $^{2}\Delta C^{\alpha}(ND)$ for $^{15}N_i$ and to $^{3}\Delta C^{\alpha}(ND)$ for $^{15}N_{i+1}$. As the HCA(CO)N experiment yields higher sensitivity than the HCAN experiment, $^{3}\Delta C^{\alpha}(ND)$ isotope shifts are measured from the HCA(CO)N spectrum, whereas $^{2}\Delta C^{\alpha}(ND)$ values are measured from the HCAN spectrum. Note that the $^{13}C^{\alpha}_i-^{15}N_i$ and $^{13}C^{\alpha}_i-^{15}N_{i+1}$ correlations are broadened in the $^{13}C^{\alpha}$ dimension by the (unresolved) $^{3}\Delta C^{\alpha}(ND)$ and $^{2}\Delta C^{\alpha}(ND)$ isotope shifts, respectively. As $^{2}\Delta C^{\alpha}(ND) > {}^{3}\Delta C^{\alpha}(ND)$, $^{13}C^{\alpha}_i-^{15}N_{i+1}$ correlations have slightly larger line widths in the $^{13}C^{\alpha}$ dimension than the $^{13}C^{\alpha}_i-^{15}N_i$ correlations (Figure 2).

Each 3D spectrum was recorded twice, and the pairwise root-mean-square difference (rmsd) between the two measurements was 4.9 ppb for $^{2}\Delta C^{\alpha}(ND)$ and 2.0 ppb for $^{3}\Delta C^{\alpha}(ND)$. This indicates random uncertainties of 2.5 and 1.0 ppb in their

(30) Zhu, G.; Bax, A. *J. Magn. Reson.* **1990**, *90*, 405−410.
(31) Griesinger, C.; Sørensen, O. W.; Ernst, R. R. *J. Am. Chem. Soc.* **1985**, *107*, 6394−6396.
(32) Montelione, G. T.; Winkler, M. E.; Rauenbuehler, P.; Wagner, G. *J. Magn. Reson.* **1989**, *82*, 198−204.
(33) Biamonti, C.; Rios, C. B.; Lyons, B. A.; Montelione, G. T. *Adv. Biophys. Chem.* **1994**, *4*, 51−120.
(34) Eberstadt, M.; Gemmecker, G.; Mierke, D. F.; Kessler, H. *Angew. Chem., Int. Ed. Engl.* **1995**, *34*, 1671−1695.
(35) Delaglio, F.; Torchia, D. A.; Bax, A. *J. Biomol. NMR.* **1991**, *1*, 439−446.
(36) LiWang, A. C.; Bax, A. *J. Am. Chem. Soc.* **1996**, *118*, 12864−12865.

averaged values, respectively, which are presented in Table 1. Measured $^2\Delta C^{\alpha}(ND)$ values are less precise than $^3\Delta C^{\alpha}(ND)$ because of the lower signal-to-noise ratio of the HCAN spectrum over that of the HCA(CO)N spectrum.

Correlation between $^3\Delta C^{\alpha}(ND)$ and ψ. Because of the more striking, relatively simple dependence of the three-bond isotope shift on ψ, we shall discuss this case first. Values for $^3\Delta C^{\alpha}(ND)$ were obtained for all residues except for Gly and residues followed by Pro (Table 1). Glycine residues do not yield observable correlations in the HCAN and HCA(CO)N spectra because the corresponding pulse schemes include $^{13}C^{\alpha}$-$\{^1H^{\alpha}\}$ refocusing delays that have been optimized for methine groups, and the Rance−Kay style gradient enhanced detection is also optimized for methine sites.

Figure 3 shows the values of $^3\Delta C^{\alpha}(ND)$ as a function of the backbone ψ angle, taken from the 1.8 Å X-ray structure of ubiquitin.[23] The data show a sinusoidal dependence on ψ, although it is also clear that residues with a positive ϕ angle (marked "+" in Figure 3) and residues followed by Gly ("o" in Figure 3) have considerably lower values than other residues with similar ψ angles (see Discussion section). These residues, and the flexible C-terminal residues, Arg^{72}−Gly^{76}, were not considered when calculating the least squares best-fit between the measured $^3\Delta C^{\alpha}(ND)$ values and the function $^3\Delta C^{\alpha}(ND) = A + B\sin(\psi)$, yielding

$$^3\Delta C^{\alpha}(ND) = 30.1 + 22.2\sin(\psi)\ \text{ppb} \quad (1)$$

The rmsd between measured isotope shifts and and those predicted by eq 1 equals 3.4 ppb. The rmsd drops by a statistically insignificant amount, 0.05 ppb, when fitting the data to $^3\Delta C^{\alpha}(ND) = A + B\sin(\psi+D)$, for $D = -4°$. When fitting a (ϕ,ψ)-dependent function to the data, including residues with positive ϕ angles (but not Met 1, for which ϕ is not defined), the following function is obtained:

$$^3\Delta C^{\alpha}(ND) = 25.4 - 5.6\sin(\phi-24°) + 20.6\sin(\psi-7°)\ \text{ppb} \quad (2)$$

Here, the rmsd between measured and predicted isotope shifts equals 3.3 ppb. Thus, this fit is of the same quality as the simple ψ-dependent fit of eq 1, which does not include residues with positive ϕ angles. However, the magnitude of the ϕ-dependent term in eq 2 is determined almost exclusively by the two residues with a positive ϕ angle (the third residue with a positive ϕ angle, Ala^{46} is followed by Gly and therefore not considered in the fit). When excluding these two residues, eq 2 yields no significant improvement in the fit over use of eq 1, indicating that eq 2 should be interpreted with caution.

$^2\Delta C^{\alpha}(ND)$ and Backbone Geometry. Two-bond isotope shifts, $^2\Delta C^{\alpha}(ND)$, range from 70 to 116 ppb. Because the number of resonances in the HCAN spectrum is 2-fold larger, there are a significant number of residues for which no reliable value could be obtained as a result of spectral overlap. Note that the intraresidual and sequential peaks are only dispersed in the ^{15}N dimension (Figure 2A), and a minimum 1.5 ppm separation between $^{15}N_i$ and $^{15}N_{i+1}$ chemical shifts is required for reliable measurement of $^2\Delta C^{\alpha}(ND)$. Thus, $^2\Delta C^{\alpha}(ND)$ values were obtained for only 52 well-resolved, non-Gly, non-Pro residues (Table 1). A best fit of the data to $^2\Delta C^{\alpha}(ND) = A + B\sin(\phi+C) + D\sin(\psi+E)$ yields

$$^2\Delta C^{\alpha}(ND) = 93.1 + 10.1\sin(\phi+62°) + 12.0\sin(\psi+42°)\ \text{ppb} \quad (3)$$

Table 1. Deuterium Isotope Shifts in Human Ubiquitin

residue	$^2\Delta C^{\alpha}(ND)$ (ppb)	$^3\Delta C^{\alpha}(ND)$ (ppb)	ϕ^b (deg)	ψ^b (deg)	sec struct.[c]
M1		35		150	β
Q2	90	50	−91	138	β
I3	75	36	−131	163	β
F4	77	44	−116	140	β
V5	94	47	−118	114	β
K6	88	45	−95	127	β
T7	77	34	−100	171	β
L8	96	29	−73	−7	
T9	98	18	−101	15	
G10			77	16	
K11	99[a]	42	−96	138	
T12	86	51	−120	132	β
I13	88	46	−109	142	β
T14	88	43	−101	140	β
L15	86	44	−126	154	β
E16	86	51	−112	121	β
V17	70	33	−139	171	β
E18	83		−120	144	
P19		19	−55	−24	
S20	98	22	−80	−8	
D21	105[a]	47	−71	148	
T22	90	35	−84	160	
I23	83[a]	19	−61	−37	α
E24	101[a]	14	−58	−40	α
N25	95	14	−65	−44	α
V26	91	15	−58	−46	α
K27	95	16	−61	−38	α
A28	96	20	−66	−38	α
K29	92	18	−64	−37	α
I30	87	16	−70	−40	α
Q31	98	15	−62	−49	α
D32	105[a]	16	−53	−42	α
K33	96	20	−94	−24	α
E34	85	18	−124	−6	α
G35			81	5	
I36	94		−80	125	
P37			−57	137	
P38		18	−57	−32	3_{10}
D39	95	22	−68	−16	3_{10}
Q40	85[a]	23	−96	−10	3_{10}
Q41	90	51	−85	130	β
R42	98[a]	52	−121	116	β
L43	87	49	−104	130	β
I44	86	39	−122	132	β
F45	100	47	−144	130	β
A46	113	29	48	46	
G47			62	22	
L48	65[a]	38	−115	143	β
Q49	89	47	−86	130	β
L50	88	48	−80	138	
E51	83	47	−102	140	
D52	91[a]	9	−48	−42	
G53			−83	−9	
R54	83	44	−86	165	
T55	83	30	−104	165	
L56	94	17	−61	−36	
S57	94	13	−64	−30	3_{10}
D58	95	22	−56	−39	3_{10}
Y59	85[a]	26	−91	5	3_{10}
N60	116	30	58	45	
I61	93	52	−89	116	
Q62	85	32	−103	169	
K63	95	45	−55	143	
E64	109	28	67	19	
S65	91	42	−71	159	
T66	90	53	−119	127	β
L67	71	40	−103	155	β
H68	84	41	−106	136	β
L69	90	49	−107	116	β
V70	86	40	−108	140	β
L71	nd[a]	43	−96	139	β
R72	73[a]	43	−118	99	
L73	99	38	*d*	*d*	
R74	97	35	*d*	*d*	

[a] Value is somewhat uncertain due to partial overlap and therefore has not been used for deriving eq 3. "nd" stands for "not determined due to severe overlap". [b] Angles are taken from the crystal structure.[16] [c] Secondary structure is identified by the program MOLMOL.[49] [d] The C-terminal residues (including G75 and G76 for which no values have been measured) are dynamically disordered in solution.[48]

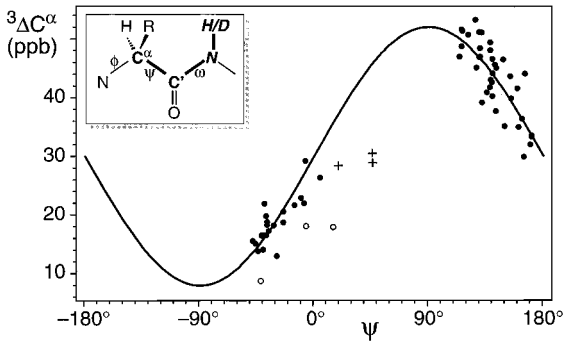

Figure 3. Plots of $^3\Delta C^\alpha$(ND) *versus* ψ. Data were obtained from the HCA(CO)N spectrum. The best fit to the data is shown as a solid line and corresponds to eq 1 (see text). Residues with positive ϕ angles and residues followed by Gly (position $i+1$) are represented by "+" and "o", respectively, and these residues are not used for deriving eq 1.

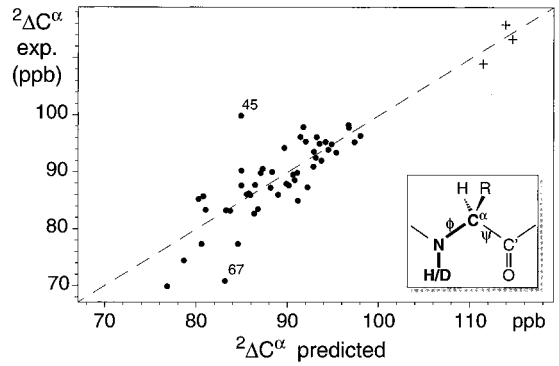

Figure 4. Plot of the $^2\Delta C^\alpha$(ND) values measured in human ubiqutin *versus* values predicted by eq 3, using X-ray crystal structure ϕ and ψ angles. Experimental data were obtained from the HCAN spectrum. Residues with a positive ϕ angle are marked "+".

This correlation is shown in Figure 4, and the rmsd between measured and predicted shifts equals 4.1 ppb. As can be seen in this figure, $^2\Delta C^\alpha$(ND) values for residues with positive ϕ angles, marked "+", are considerably larger than those for residues with negative ϕ angles.

$^2\Delta C^\alpha$(ND) and Hydrogen Bonding. Based on the study of small model compounds, it was expected that $^2\Delta C^\alpha$(ND) increases with the strength of the amide hydrogen bond.[12] Although the strength of hydrogen bonds in proteins is difficult to evaluate from a crystal structure solved at 1.8 Å resolution, downfield amide proton shifts, $\delta(H^N)$, are commonly interpreted in terms of strong hydrogen bonding.[37] However, a plot of $^2\Delta C^\alpha$(ND) versus amide proton chemical shift shows that, on average, there appears to be a small *decrease* of $^2\Delta C^\alpha$(ND) with increasing amide proton chemical shift, *i.e.*, with increasing hydrogen bond strength (Supporitng Information). However, the plot shows a large amount of scatter and does not meet the statistically required criteria for establishing such a correlation ($p = 0.12$). The same applies when the geometric dependence of eq 3 is subtracted from the measured $^2\Delta C^\alpha$(ND) values, prior to plotting its value against $\delta(H^N)$ (Supporting Information).

Discussion

$^3\Delta C^\alpha$(ND). Our results for $^3\Delta C^\alpha$(ND) must clearly be distinguished from the earlier finding that three-bond isotope shifts are correlated with the dihedral angle defined by the three intervening bonds.[5,9] In our case, this dihedral angle is the peptide bond angle, ω, which equals 180° for *trans* peptide bonds, and rms devations from planarity are smaller than *ca.* 5°.[38,39] Therefore, the $C^\alpha_i-C'_i$ bond is *cis* to the $N_{i+1}-H/D$ bond, and therefore a uniform, maximum three-bond isotope effect would be expected for all $^{13}C^\alpha$ nuclei preceding a *trans* peptide bond.[5,9] The finding that these effects are also strongly influenced by dihedral angles that do not change the relative positions of the atoms of interest is unique so far and sheds new light on the subject. Clearly, ψ influences the electron distribution around C^α_i with respect to NH/D_{i+1}. Presumably, this forms the basis for the effects observed.

All $^3\Delta C^\alpha$(ND) values for α-helical residues in ubiquitin fall below 21 ppb, whereas all β-sheet values are larger than 33 ppb (Table 1). In contrast to the use of secondary $^{13}C^\alpha$ or $^1H^\alpha$ shifts, which are commonly used for identifying secondary structure,[40,41] there is a wide separation between the range of α-helical and β-sheet $^3\Delta C^\alpha$(ND) values. Thus, $^3\Delta C^\alpha$(ND) appears to be a very clear marker for secondary structure, and, more importantly, it provides very direct information on the ψ angle. As eq 1 is 30° out of phase relative to the ψ-dependent $H^\alpha_i-H^N_{i+1}$ distance curve,[42] information contained in $^3\Delta C^\alpha$-(ND) complements that contained in $H^\alpha_i-H^N_{i+1}$ NOEs.

Interestingly, the magnitude of $^3\Delta C^\alpha$(ND) appears to be reduced by about 10 ppb if the sequential residue is a Gly. This indicates that $^3\Delta C^\alpha_i$(ND) is influenced by more than ψ_i alone and suggests that it also depends weakly on the type and conformation of residue $i+1$. Similarly, there may be a weak correlation with the type and conformation of the side chain of residue i. The number of $^3\Delta C^\alpha$(ND) values measured in ubiquitin is far too small for analyzing such effects, but it is likely that they are significant contributors to the residual 3.4 ppb rmsd between eq 1 and the measured values.

$^2\Delta C^\alpha$(ND). The value of $^2\Delta C^\alpha$(ND) also depends strongly on the backbone conformation and is a function of both ϕ and ψ. Although $^2\Delta C^\alpha$(ND) values for α-helical and β-sheet secondary structure partially overlap, they nevertheless are useful reporters for local backbone geometry. The range of $^2\Delta C^\alpha$-(ND) values is more than 10-fold larger than the rmsd between measured values and those predicted by eq 3. This is comparable to the deviations between, for example, measured $^3J_{HNH\alpha}$ and $^1J_{C\alpha H\alpha}$ couplings and their empirically predicted values.[43,44] Therefore, $^2\Delta C^\alpha$(ND) values may also be useful for structure refinement, and, even while $^2\Delta C^\alpha$(ND) depends on both ϕ and ψ, it is straightforward to generate a (ϕ,ψ)-dependent energetic penalty function which minimizes the difference between measured $^2\Delta C^\alpha$(ND) values and those predicted by eq 3 during structure calculations. Such a procedure is fully analogous to routines previously described for the X-PLOR[45] structure calculation program and which have been used to refine structures directly against measured J couplings.[46]

The three non-Gly residues in ubiquitin with positive ϕ angles all have significantly larger $^2\Delta C^\alpha$(ND) values (>108 ppb) than

(37) Wagner, G.; Pardi, A.; Wüthrich, K. *J. Am. Chem. Soc.* **1983**, *105*, 5948−5949.
(38) MacArthur, M. W.; Thornton, J. M. *J. Mol. Biol.* **1996**, *264*, 1180−1195.
(39) Hu, J.-S.; Bax, A. *J. Am. Chem. Soc.* In press.
(40) Wishart, D. S.; Sykes, B. D.; Richards, F. M. *J. Mol. Biol.* **1991**, *222*, 311−333.
(41) Spera, S.; Bax, A. *J. Am. Chem. Soc.* **1991**, *113*, 5490−5492.
(42) Wüthrich, K. *NMR of Proteins and Nucleic Acids*; Wiley: New York, 1986.
(43) Pardi, A.; Billeter, M.; Wüthrich, K. *J. Mol. Biol.* **1984**, *180*, 741−751.
(44) Vuister, G. W.; Delaglio, F.; Bax, A. *J. Am. Chem. Soc.* **1992**, *114*, 9674−9675.
(45) Brünger, A. T. *X-PLOR Version 3.1: A System for X-ray Crystallography and NMR*; Yale University Press: New Haven, CT, 1992.
(46) Garrett, D. S.; Kuszewski, J.; Hancock, T. J.; Lodi, P. J.; Vuister, G. W.; Gronenborn, A. M.; Clore, G. M. *J. Magn. Reson. B.* **1994**, *104*, 99−103.

residues with negative ϕ angles. This indicates that $^2\Delta C^{\alpha}(ND)$ potentially could be a useful indicator for identifying such residues in an unbiased manner.

For two residues (Phe[45] and Leu[67]) $^2\Delta C^{\alpha}(ND)$ differs by more than two standard deviations from the value predicted by the empirical eq 3. Leu[67] has the second smallest $^2\Delta C^{\alpha}(ND)$ value in ubiquitin and is located near the middle of ubiquitin's fifth β-strand. It does not appear to have any exceptional features relative to other residues, such as residue type, neighboring residues, abnormal χ_1 angles, extreme chemical shifts, or extraordinary hydrogen bonding energies. Phe[45] has a considerably higher observed than predicted $^2\Delta C^{\alpha}(ND)$ value. It also represents a reliable, highly reproducible measurement. It precedes Ala[46], which has a positive ϕ angle. However, in all likelihood, the positive ϕ angle of Ala[46] is not the reason for the anomolously high $^2\Delta C^{\alpha}(ND)$ value since Tyr[59] and Lys[63], which also precede residues with positive ϕ angles, do not show such an anomolous increase. Thus, there must be additional contributions to the two-bond isotope effects of these residues that remain not understood.

Concluding Remarks

We have shown that $^2\Delta C^{\alpha}(ND)$ and $^3\Delta C^{\alpha}(ND)$ values in proteins can be readily measured using gradient-enhanced triple resonance NMR experiments. $^2\Delta C^{\alpha}(ND)$ values are influenced by both the intraresidue ϕ and ψ angles and do not show a statistically significant dependence on hydrogen bond strength. To the best of our knowledge no *ab initio* results have been published for $^2\Delta C^{\alpha}(ND)$ in peptide systems. It is anticipated that such calculations will shed additional light on the various factors influencing $^2\Delta C^{\alpha}(ND)$.

Of particular interest are the three-bond effects: distinct from earlier descriptions of a dependence on the dihedral angle formed by the three bonds,[5,9] *i.e.*, rotations around the second bond, we find that these effects are also very sensitive to rotations around the third bond: In polypeptides, changes in $^3\Delta C^{\alpha}(ND)$ are strongly correlated with the backbone torsion angle ψ. $^3\Delta C^{\alpha}(ND)$ therefore provides a unique possibility to evaluate ψ angles in proteins. In contrast to the backbone torsion angle ϕ, which is characterized by six readily measurable J couplings,[26,39] only a single J coupling ($^3J_{H\alpha N}$) is available for ψ, and this coupling is too small to be of much practical use in medium size proteins.[47] The simple sinusoidal dependence on ψ, and the lack of additional, quadratic terms as found in J coupling Karplus curves, causes the model function (eq 1) to be only 2-fold degenerate. This contrasts with the 4-fold degeneracy of Karplus curves and makes its use in structure calculation less prone to error. Therefore, $^3\Delta C^{\alpha}(ND)$ potentially is a very useful parameter in NMR protein structure determination. In favorable cases, it is feasible to obtain $^3\Delta C^{\alpha}(ND)$ measurements also from a sample containing only 10−15% D_2O, commonly used for most other types of triple resonance NMR experiments, avoiding the need to prepare a separate sample.

Our results show that two- and three-bond isotope shifts strongly depend on local geometry. Relations analogous to the ones derived here for $^{2,3}\Delta C^{\alpha}(ND)$ are expected to apply for deuteration of side-chain resonances. Once such relations have been established, it is conceivable that the magnitudes of deuterium isotope effects on ^{13}C and ^{15}N chemical shifts may become of considerable use in determining the structure of both the backbone and the side chains of fractionally deuterated proteins.

Acknowledgment. We thank Nico Tjandra for helpful discussions and Frank Delaglio and Dan Garrett for assistance and use of their software. This work was supported by the AIDS Targeted Anti-Viral Program of the Office of the Director of the National Institutes of Health. M.O. is supported by a Swiss National Science Foundation post-doctoral fellowship.

Supporting Information Available: Pulse diagrams and parameters for the HCAN and HCA(CO)N experiments without gradient enhancement; a plot of $^2\Delta C^{\alpha}(ND)$ values *versus* H^N chemical shift; and a plot of the difference between the observed $^2\Delta C^{\alpha}(ND)$ values and those predicted by eq 3 *versus* H^N chemical shift (4 pages). See any current masthead page for ordering and Internet access instructions.

JA9707466

(47) Wang, A. C.; Bax, A. *J. Am. Chem. Soc.* **1995**, *117*, 1810−1813.
(48) Tjandra, N.; Feller, S. E.; Pastor, R. W.; Bax, A. *J. Am. Chem. Soc.* **1995**, *117*, 12562−12566.
(49) Koradi, R.; Billeter, M.; Wüthrich, K. *J. Mol. Graphics* **1996**, *14*, 52−55.